Heterogeneous Hydrolysis and Reaction of $BrONO_2$ and Br_2O on Pure Ice and Ice Doped with HBr

Arnaud Aguzzi and Michel J. Rossi*

Laboratoire de Pollution Atmosphérique (LPA), Sciences et Ingénierie de l'Environnement (SIE), École Polytechnique Fédérale de Lausanne (EPFL), CH-1015 Lausanne, Switzerland

Received: November 30, 2001; In Final Form: March 19, 2002

The rate of uptake of bromine nitrate ($BrONO_2$) and dibromine monoxide (Br_2O) on different types of ice, such as condensed (C), bulk (B), and single-crystal ice (SC) have been investigated in a Teflon-coated Knudsen flow reactor in the temperature range 180−210 K using mass spectrometric detection. For the whole temperature range the Br_2O uptake kinetics is first order in [Br_2O] with a mean initial uptake coefficient of $\gamma_0 = 0.24 \pm 0.10$, which leads to the exclusive formation of HOBr. The $BrONO_2$ hydrolysis has been measured on B-, C-, and SC-type ice and leads to HOBr and Br_2O on all types of ice. At a fixed temperature the rate law is first order in [$BrONO_2$] with $\gamma \approx 0.3$ at 180 K. The observed negative temperature dependence for the heterogeneous hydrolysis of $BrONO_2$ on pure ice leads to E_a of -2.0 ± 0.2, -2.1 ± 0.2, and -6.6 ± 0.3 kcal/mol on C-, B- and SC-type ice, respectively. Despite the high reactivity of $BrONO_2$ on ice substrates, the kinetics of interaction of $BrONO_2$ on ice nevertheless depends on the type of ice used. No saturation of the uptake coefficient has been observed during the $BrONO_2$ hydrolysis on ice in contrast to the $ClONO_2$/ice system. On ice samples doped with approximately 5×10^{16} molecules HBr per cm^3 the kinetics of the interaction of $BrONO_2$ with HBr leads to an uptake coefficient similar to that for $BrONO_2$ hydrolysis. The interaction of $BrONO_2$ with HBr occurs via the hydrolysis of $BrONO_2$ to HNO_3 and HOBr where the latter reacts with HBr in a fast secondary reaction to produce Br_2 with $E_a = -1.2 \pm 0.2$ kcal/mol.

Introduction

Polar stratospheric cloud (PSC) particles are now well recognized as sites of heterogeneous reactions for various chlorine- and bromine-containing molecules leading to stratospheric ozone depletion over the polar regions through release of photochemically labile species.[1−7]

Bromine nitrate, $BrONO_2$, an important halogen and NO_x reservoir, is known to be formed in the atmosphere via the homogeneous recombination reaction of BrO with NO_2 whose high-pressure rate coefficient has been measured as $k_\infty = 1.4 \times 10^{-11}$ $(T/300)$ cm^3 $molecule^{-1}$ s^{-1} in the temperature range 248−346 K.[8] Other laboratory investigations involving $BrONO_2$ have focused on the measurement of its absorption cross section[9,10] and photodissociation quantum yields.[11] It leads to the formation of Br + NO_3 (λ < 900 nm) or BrO + NO_2 (λ < 1100 nm) depending on the photolysis wavelength. It had been thought that gas-phase reactions of $BrONO_2$ with Br, Cl or O(^{3}P) were not important which is why these reactions received little attention. However, as described by Soller et al.[12] the gas-phase reaction of $BrONO_2$ with O(^{3}P) appears to be important under stratospheric conditions and should be included in models of stratospheric chemistry in contrast to the gas-phase reaction of $ClONO_2$ + O(^{3}P), which has a negligible contribution toward the lower stratospheric destruction of $ClONO_2$.[13]

Another sink of $BrONO_2$ may be the heterogeneous hydrolysis on ice, which is the focus of the present paper. Recent mechanistic studies of this system led to the conclusion that the reaction proceeds by an ionic mechanism to result in the hypobromous ion BrO^-.[14,15] Laboratory kinetic studies of the heterogeneous hydrolysis of $BrONO_2$ [16−18] have shown that the reaction readily occurs on ice surfaces according to reaction 1 with an uptake coefficient of the order of 0.2 at 190 K:[18]

$$BrONO_2(g) + H_2O(s) \rightarrow HOBr(g) + HNO_3(s) \quad (1)$$

The hydrolysis of $BrONO_2$ on ice surfaces promptly leads to the formation of HOBr and HNO_3, which means that this chemistry is efficient in converting NO_x to NO_y species.[17] As a consequence a significant amount of OH will be produced in the lower stratosphere through HOBr photolysis, leading to OH + Br. The released gaseous HOBr may thus be rapidly converted to active bromine by photolysis[19] or by heterogeneous reactions with solvated halide ions X^- according to[18,20]

$$HOBr(g) + X^- \rightarrow BrX(g) + OH^- \quad (2)$$

Allanic et al.[18] observed Br_2O as a secondary product during $BrONO_2$ uptake on ice according to reaction 3 in analogy to Cl_2O formation at excess $ClONO_2$ in the presence of ice.[21] This

$$BrONO_2(g) + HOBr(a) \rightarrow Br_2O(g) + HNO_3(s) \quad (3)$$

latter reaction complicates the monitoring of the hydrolysis of $BrONO_2$ on ice since both $BrONO_2$ and Br_2O contribute to the BrO^+ fragment at *m*/*e* 95 which we used to monitor $BrONO_2$.[22]

For the gas-phase hydrolysis reaction of Br_2O (reaction 4) and Cl_2O (reaction 5) the equilibrium constants of 0.02[19] and 0.09[23] have been measured at 300 K, respectively. Standard enthalpies of formation and absolute entropies of X_2O, HOX (X = Cl, Br) and H_2O are displayed in Table 1 and lead to

* To whom correspondence should be addressed. E-mail: michel.rossi@epfl.ch.

10.1021/jp014383e CCC: $22.00
Published on Web 05/24/2002

TABLE 1: Enthalpies of Formation [kcal/mol] and Standard Entropies [cal/(mol·K)] of Br_2O, HOBr, Cl_2O, HOCl, and H_2O

compounds	$\Delta_f H^0_{298}$	S^0_{298}
Br_2O	25.6 ± 0.8[a]	78.15[f]
HOBr	-14.3 ± 0.8[b]	59.20[g]
Cl_2O	18.5 ± 0.8[c]	64.00[g]
HOCl	-18.4 ± 0.8[d]	56.50[g]
H_2O	-57.811 ± 0.009[e]	45.01[g]

[a] Derived from the heat of formation of BrO^+ and Br.[37] [b] Estimated.[37,38] [c] Derived from the heat of formation of ClO^+ and Cl.[39] [d] Estimated.[39] [e] Reference 40. [f] $S^0_{298} = \dfrac{\Delta_f H^0_{298} - RTln(K_{eq})}{T}$. [g] Reference 41.

TABLE 2: Knudsen Cell Parameters

parameter	value
volume of the reactor, V	1830 cm^3
estimated surface area (total)	1300 cm^2
sample surface area, A_s	17 cm^2
gas noumber concentration, [C][a]	$(1-1000) \times 10^9$ cm^{-3}
surface collision frequency, ω[b]	$\omega = 2A_s(T/M)^{1/2}$ s^{-1}
escape rate constant, k_{esc} [c]	
for the 8 mm orifice	$0.80(T/M)^{1/2}$ s^{-1}
for the 14 mm orifice	$1.77(T/M)^{1/2}$ s^{-1}

[a] Calculated using the relation $F^i = Vk_{esc}[C]$, where F^i is the flow entering the cell and [C] is the concentration. [b] T and M are the temperature and the molecular weight, respectively. [c] Value determined by experiment.

standard heats of reaction of +3.5 kcal/mol for reaction 4 and +2.6 kcal/mol for reaction 5.

$$Br_2O + H_2O \leftrightarrows 2HOBr \qquad \Delta_r H^0_{298} = +3.5 \text{ kcal /mol} \qquad (4)$$

$$Cl_2O + H_2O \leftrightarrows 2HOCl \qquad \Delta_r H^0_{298} = +2.6 \text{ kcal /mol} \qquad (5)$$

Oppliger et al.[21] did not observe a heterogeneous interaction between Cl_2O and ice substrates even when the ice was doped with HCl. However, to date the analogous hydrolysis reaction of Br_2O occurring on ice surfaces at low temperatures relevant to the stratosphere has not been determined. This is one of the reasons that has motivated the study of the heterogeneous hydrolysis of Br_2O on ice, where for the first time the uptake kinetics of Br_2O on ice surfaces is given as well as the HOBr yields resulting from this interaction. Another motivation for these experiments is that Br_2O is often observed as an impurity in a $BrONO_2$ storage vessel, which complicates the analysis of its reaction kinetics. Knowledge on the properties of Br_2O will enable the appropriate corrections to be made.

However, the main goal of this paper is to present the uptake kinetics of the heterogeneous reaction of $BrONO_2$ with different types of ice substrates that may be relevant to the lower stratosphere, because the chemical composition of PSC particles is still somewhat uncertain.[24] The kinetics of the heterogeneous reaction of $BrONO_2$ on ice doped with HBr, leading to the formation of Br_2 and HNO_3, is also presented for the first time.

Experimental Section

Experimental Apparatus. The uptake experiments have been performed using a FEP Teflon-coated Knudsen flow reactor equipped with a mass spectrometer (MS) described elsewhere.[25] The characteristic parameters of the reactor are presented in Table 2. The experiments described in this study are based on two different types of protocols. The first one is a pulsed valve (PV), and the second a steady-state (SS) experiment.

In a PV experiment the gas is introduced into the flow reactor through the pulsed valve at pulse lengths of a few milliseconds. Typical doses range from 10^{13} to 10^{16} molecules per pulse. When the sample chamber is closed, the reactant decay of the MS signal of the so-called reference pulse corresponds to k_{esc}, the escape rate constant for effusion of molecules from the flow reactor. The reactive pulse is obtained by admitting an identical quantity with the sample exposed to the flow. The decay of this MS signal, which is a primary observable in a PV experiment, is given by k_{dec} and corresponds to the sum of k_{uni}, the reaction rate constant of interest, and k_{esc} according to eq 6.

$$k_{dec} = k_{uni} + k_{esc} \qquad (6)$$

The PV experiment causes a transient supersaturation that enables kinetic studies in real time by the measurement of the gas lifetime in the reactor. We also obtain the time dependent rate of formation of the reaction products by monitoring the corresponding MS signal during and just after injection of the reactant. The PV experiments are useful for the study of the mechanism of the reaction, since short-lived intermediates may be detected. A typical PV experiment is shown in Figure 1.

A typical SS experiment involves introducing a constant flow of gas through a capillary into the Knudsen flow reactor. When steady state is established, the movable plunger is lifted; thus the reactive condensed phase is exposed to the flowing gas and the rate of uptake may be measured. The change in the MS signal upon opening and closing the sample compartment is related to k_{uni}, which is a primary observable in SS experiments. We assume that the rate law for uptake is first order in the reactant and calculate the value of the rate constant, k_{uni}, according to eq 7,[25] where I_0 and I are the intensities of the

$$k_{uni} = k_{esc}\frac{I_0 - I}{I} \qquad (7)$$

steady-state MS signal levels before and during reaction. A typical SS experiment is presented in Figure 2.

The uptake coefficient γ is obtained according to eq 8, where ω is the collision frequency of the gas with the reactive surface and is calculated from gas kinetic theory (see Table 2) to result

$$\gamma = \frac{k_{uni}}{\omega} \qquad (8)$$

in $\omega = 50$ and 44 s^{-1} for $BrONO_2$ and Br_2O, respectively, at $T = 300$ K on the basis of the geometric surface area of the sample.

Gaseous Reactants. Dibromine monoxide, Br_2O, was synthesized from the reaction of Br_2 with excess HgO, in analogy to the Cl_2/Cl_2O system according to reaction 9:[26]

$$2Br_2 + HgO \rightarrow Br_2O + HgBr_2 \qquad (9)$$

Approximately 50 g of HgO powder was placed in a 2 l flask equipped with an in- and outlet valve, which was evacuated to a pressure of approximately 40 mbar. Br_2 was degassed and dried over P_2O_5. The flask was subsequently filled with 130 mbar of Br_2. After waiting for 5 min for the reactants and products to come to equilibrium, the gases were pumped through a second trap kept at 77 K. This process was repeated several times to obtain sufficient quantities of BrOBr collected in the cold trap at 77 K. The temperature of the trap was subsequently raised to approximately 200 K and Br_2 was removed by pumping. Toward the end of the pumping period of 6−9 h, a brown powder remained in the trap at 200 K. The base peak at

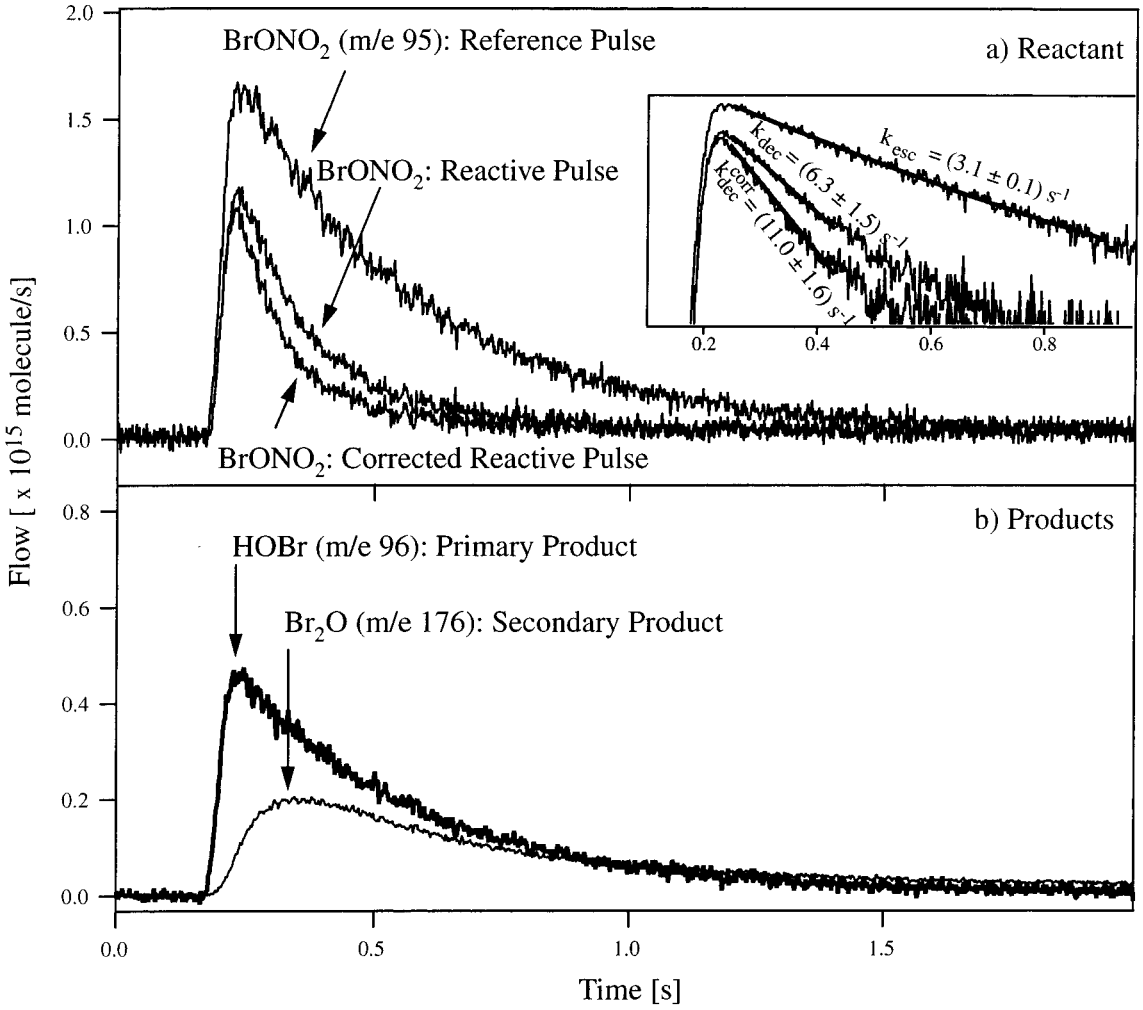

Figure 1. Pulsed valve experiment of $BrONO_2$ on condensed (C) ice at 210 K in the 14 mm aperture reactor. Panel a) shows the reactant pulses where the reference pulse corresponds to the decay of the MS signal at *m/e* 95 in the absence of ice, the reactive pulse corresponds to the same pulse in the presence of the ice sample, and the corrected $BrONO_2$ reactive pulse corresponds to the reactive pulse corrected for the Br_2O contribution at *m/e* 95 (see text). The insert in panel a) shows the decays of the different pulses on a logarithmic scale with the corresponding γ value of 0.16 $\pm$ 0.03. Panel b) shows the order of appearance of the products in real time. The bold line shows the primary product HOBr monitored at *m/e* 96, while the thin line shows the secondary product Br_2O monitored at *m/e* 176.

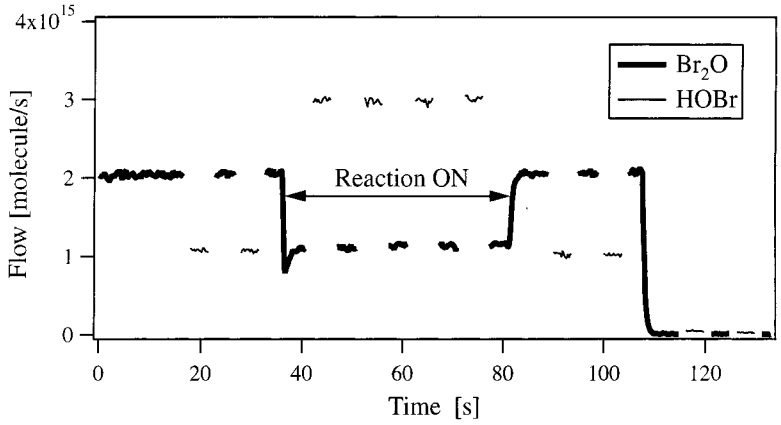

Figure 2. Steady-state experiment of Br_2O (*m/e* 176, bold line) on a C ice sample (thickness of approximately 2 μm) at 210 K in the 14 mm orifice reactor. HOBr (*m/e* 98, thin line), the sole product, appears at a 100% yield with one Br_2O resulting in two HOBr molecules.

m/e 176 (Br_2O^+) which unambiguously reveals the presence of Br_2O was chosen to monitor gaseous Br_2O. The trap also contains HOBr (*m/e* 96 and 98) and Br_2 as impurities. Important quantities of H_2O remain in the batch of Br_2O owing to water vapor absorbed on HgO. Even after prolonged pumping, the impurities remain adsorbed in the trap. The Br_2O flow rate entering the flow reactor through a 3 mm inner diameter Teflon tube is controlled by adjusting the temperature of the storage cold bath. No Br_2O has been observed at its parent peak (*m/e* 176) when the inlet used was a capillary entry probably due to a large number of collisions of Br_2O against the inner wall leading to decomposition of the Br_2O molecules.

Bromine nitrate, $BrONO_2$, is synthesized from the reaction of $ClONO_2$ with Br_2 according to reaction 10 following the procedure described by Wilson et al.[27] $ClONO_2$ is mixed with

$$ClONO_2 + Br_2 \rightarrow BrONO_2 + BrCl \qquad (10)$$

Br_2 in a molar ratio of 3:1 in a trap at 77 K. Before condensation $ClONO_2$ and Br_2 are passed across a P_2O_5 trap in order to dry the reactants.

The mixture is kept at ambient temperature for an hour and condensed in a cold trap at 200 K in a cold circulation bath during 12 h. Unreacted Br_2, $ClONO_2$, and other impurities are removed by pumping for 2−3 h at a temperature range of 200−220 K. The remaining product is a solid yellow substance. However, Br_2, BrCl, and sometimes Br_2O still remain in the trap as impurities even after long periods of pumping. The base peak is at *m*/*e* 46 (NO_2^+), but we did not use *m*/*e* 46 to monitor $BrONO_2$ in order to avoid any confusion with other species contributing to this mass. We chose to monitor $BrONO_2$ at *m*/*e* 95 (BrO^+), which is an unambiguous marker for $BrONO_2$ as long as Br_2O is either absent or present in known quantities such that an appropriate correction may be performed at *m*/*e* 95.[22] The typical ratio of *m*/*e* 46 to 95 is 20:1.

Ice Substrates. The procedures used to obtain the different ice samples are the following. "Bulk ice" (B) has been obtained by pouring liquid deionized water into the sample dish prior to any experiment. The water is then degassed by freeze−pump−thaw cycles and finally cooled to a chosen temperature in about 15 min.

To prepare "single-crystal ice" (SC) one poured liquid deionized water into the sample dish as for B samples, but the rate of cooling was much lower in the temperature range 273−240 K. The rate of temperature decrease was set to −0.3 K/min according to the procedure described by Knight.[28] At present we do not have an in situ optical characterization for SC samples, but we notice that SC ice seems more transparent to the eye than B samples. In addition, experiments performed on SC samples show distinctly different kinetics compared to the ones performed on B samples,[29] as we will see later in this paper.

"Condensed ice" (C) has been obtained by depositing water vapor in situ onto the cold support at 150 K at a background pressure of 10^{-5} Torr. The empty support is attached to the reactor and subsequently cooled to the desired temperature with the plunger lowered, that is, the sample compartment sealed off. When the chosen temperature of 150 K is reached, the plunger is lifted and the sample dish exposed to a high water flow of the order of 10^{19} molecule/s for several minutes. This results in an average sample size of about 10^5 formal monolayers (ML) of 250 nm total thickness.

Results and Discussion

The motivation to study the heterogeneous reaction of Br_2O on ice results from the fact that it is presumably formed both by the heterogeneous decomposition reaction 11 inside the

$$2BrONO_2 \rightarrow Br_2O + N_2O_5 \qquad (11)$$

$BrONO_2$ storage vessel and by the fast secondary heterogeneous reaction 3 taking place inside the flow reactor in the presence of ice.[22]

The similarity of the mass spectral signature between Br_2O and $BrONO_2$ makes it difficult to obtain an unambiguous marker for $BrONO_2$, the molecule of interest. We have therefore elected to study the behavior of Br_2O in the presence of an ice substrate in order to better characterize $BrONO_2$, which may be contaminated by variable amounts of Br_2O.

Br_2O on Ice. Steady-state (SS) experiments on bulk (B) and condensed (C) ice have been performed in the 14 mm orifice reactor in the temperature range 180−210 K. Br_2O, monitored at its parent peak at *m*/*e* 176 reacts on fresh ice surfaces to hypobromous acid, HOBr, monitored at *m*/*e* 98 (or 96), according to the following reaction:

$$Br_2O(g) + H_2O(s) \rightarrow 2HOBr(g) \qquad (12)$$

Figure 2 displays a typical SS experiment performed at 210 K on a C ice sample. When the C ice is exposed to Br_2O a rapid drop of the signal at *m*/*e* 176 is observed (bold line), which is correlated with a rapid increase of HOBr (thin line). Right after the opening of the sample compartment at $t = 37$ s, rapid uptake of Br_2O is observed followed by a slightly smaller steady-state uptake owing to partial surface saturation.

A totally different interpretation of the Br_2O and HOBr MS signal levels may be attempted if one asserts that the steady-state levels for both MS signals are given by the homogeneous gas-phase equilibrium (12). This implies that the ice substrate merely acts as a catalyst that enables the establishment of an equilibrium on the time scale of a second corresponding to the "spike" in the Br_2O uptake at $t = 37$ s in Figure 2. We calculate an equilibrium constant of $K = 1.9 \times 10^{-5}$ at 210 K using the values of the thermodynamic parameters of Table 1. With $[Br_2O]$ and $[H_2O]$ equal to 5.2×10^{11} from Figure 2 and 2.4×10^{14} molecule/cm^3 from ref 29, respectively, for the Knudsen flow reactor conditions, we compute $[HOBr] = 4.9 \times 10^{10}$ molecule/cm^3, which is 1 order of magnitude lower than the value given in Figure 2 of 3.8×10^{11} molecule/cm^3. We are therefore led to conclude that the present kinetic interpretation in terms of a heterogeneous reaction is valid and that the establishment of the equilibrium does not occur on the time scale of tens of seconds at 210 K.

In the example displayed in Figure 2, the initial uptake rate constant k_0 and uptake coefficient γ_0 were measured as 4.4 s^{-1} and 0.10, respectively, whereas the corresponding steady-state values were $k_{ss} = 1.8$ s^{-1} and $\gamma_{ss} = 0.04$, respectively. Figure 3 displays the Arrhenius representation of the initial uptake rate constant k^0_{uni} as well as the steady-state rate constant k^{ss}_{uni} of Br_2O on C (full symbols) and B (open symbols) ice. The initial uptake coefficient γ_0 is constant over the whole temperature range 180−210 K with a mean value of $\gamma_0 = 0.24 \pm 0.10$, where the uncertainty is 2σ. Partial saturation of the B and C ice substrates has been observed over the whole temperature range 180−210 K and leads to a mean steady-state uptake coefficient $\gamma_{ss} = 0.04 \pm 0.02$ independent of temperature (Figure 3). The data for both the initial and steady-state rate constants are consistent with an activation energy of $E_a = 0.0 \pm 2.0$ kcal/mol. The results on the uptake kinetics of Br_2O on C and B ice are displayed in Table 3. At a fixed temperature one may conclude that the Br_2O uptake follows a first-order rate law.

HOBr has been observed as the only product of the heterogeneous hydrolysis of Br_2O. Figure 4 displays the HOBr yield as a function of temperature. The observed product yield increases with temperature from 20−40% at 180 K to 100% at 210 K. This is most certainly due to the strong interaction of HOBr on ice samples at low temperature.[30,31] At 180 K, the observed HOBr yield is approximately 30%. Assuming that the total amount of Br_2O taken up is converted to HOBr, the observed signal of HOBr is expected to be 3 times higher than the observed one. From this ratio of 3 at 180 K, one may

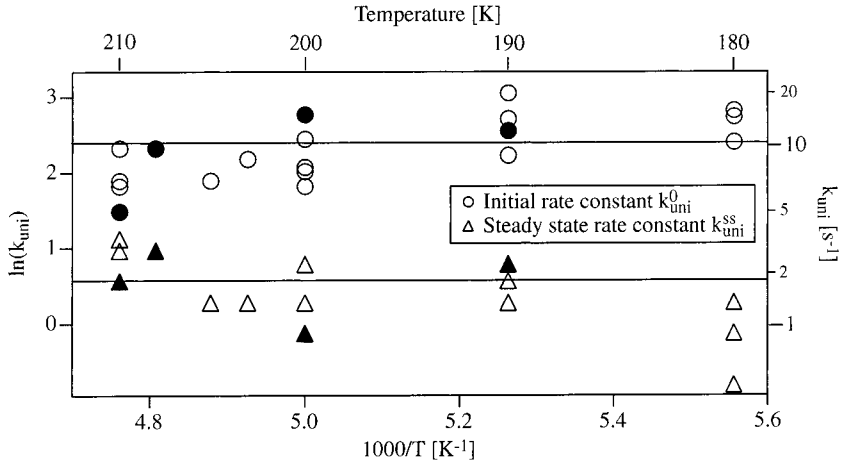

Figure 3. Arrhenius representation of the initial (circles) and steady-state (triangles) uptake rate constant k_{uni} of Br_2O interacting on B ice (open symbols) and C ice (full symbols) obtained in steady-state experiments using the 14 mm aperture reactor leading to an initial and steady-state activation energy of $E_a^0 = E_a^{ss} = 0.0 \pm 2.0$ kcal/mol.

TABLE 3: Steady State Experiments of Br_2O Performed on (a) Condensed (C) and (b) Bulk (B) Ice Samples in the 14 mm Orifice Reactor

T [K]	flow [molecule/s]	γ_0	γ_{ss}	HOBr yield [%]
		(a) C Ice		
190	4.8×10^{14}	0.21	0.05	n.d.[a]
200	1.5×10^{15}	0.36	0.02	80
208	3.6×10^{14}	0.23	0.06	102
210	2.0×10^{15}	0.10	0.04	98
		(b) B Ice		
180	5.5×10^{14}	0.38	0.01	52
180	8.6×10^{14}	0.35	0.02	25
180	8.7×10^{14}	0.25	0.03	n.d.[a]
190	8.1×10^{14}	0.29	0.03	85
190	1.3×10^{15}	0.34	0.04	70
190	1.5×10^{15}	0.48	0.03	n.d.
200	6.2×10^{14}	0.26	0.02	77
200	1.1×10^{15}	0.17	0.05	89
200	1.3×10^{15}	0.14	0.03	90
200	4.4×10^{15}	0.18	0.02	n.d.
203	1.9×10^{15}	0.20	0.03	92
205	2.5×10^{15}	0.15	0.03	82
210	1.5×10^{15}	0.15	n.o.[b]	80
210	1.6×10^{15}	0.14	n.o.	74
210	1.8×10^{15}	0.23	0.07	105
210	2.0×10^{15}	0.14	0.06	105

[a] n.d. = not determined. [b] n.o. = not observed.

calculate the corresponding γ of HOBr, using $\omega = 61$ s^{-1} and $k_{esc} = 3.1$ s^{-1},[31] resulting in a γ value of the order of 0.1, which corresponds to the measured uptake kinetics of HOBr on ice substrates[30,31] at 180 K. The assumption that the Br_2O taken up is converted to 2 HOBr at 100% yield is confirmed by thermal desorption experiments (TDE) where the missing HOBr is released into the gas phase at 215 ± 5 K, thus closing the bromine mass balance to an accuracy of ±20%. However, during TDE, one cannot distinguish between the following two situations: (1) the total amount of Br_2O taken up is quantitatively converted to HOBr upon uptake and is subsequently released into the gas phase during TDE; (2) a fraction or all of the Br_2O taken up is condensed without being converted to HOBr. During the temperature increase, Br_2O is converted to 2HOBr before desorption into the gas phase. In conclusion, we observe fast uptake kinetics of Br_2O on ice substrates resulting in prompt appearance of gas-phase HOBr, which is the sole product of the heterogeneous reaction. This result contrasts with the behavior of Cl_2O on ice substrates, which may be characterized as totally nonreactive.[21]

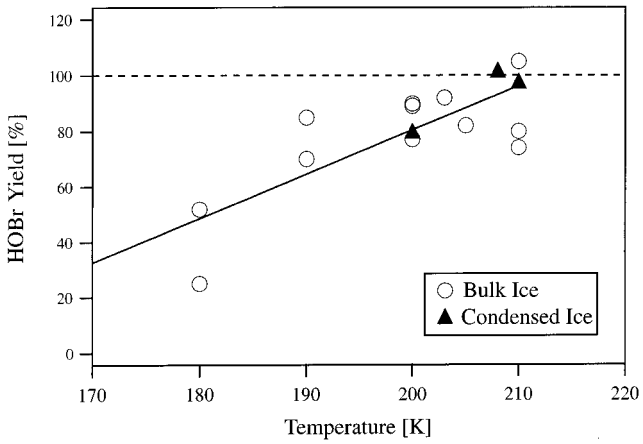

Figure 4. HOBr yield during Br_2O hydrolysis on B ice (○) and C ice (▲) as a function of temperature in the 14 mm orifice reactor.

$BrONO_2$ Uptake on Pure Ice. As mentioned before, $BrONO_2$, monitored at *m*/*e* 95, is thought to be one of the main bromine reservoir compounds in the stratosphere. It reacts on pure ice surfaces to produce hypobromous acid, HOBr, monitored at *m*/*e* 96 (or 98), according to reaction 13:[16−18]

$$BrONO_2 + H_2O \rightarrow HOBr + HNO_3 \qquad (13)$$

Throughout almost all experiments, Br_2O monitored at *m*/*e* 176 (its molecular ion peak) was present in the storage vessel as an impurity or has been formed as a secondary product during uptake on ice according to reaction 3, as has been discussed above.

Br_2O contributes to the MS signal intensity at *m*/*e* 95 to the extent of 50% of its molecular ion peak intensity at *m*/*e* 176.[22] This ratio has been used to correct the MS signal intensity at *m*/*e* 95, which could then be used to unambiguously monitor $BrONO_2$.

Figure 5 shows a typical SS experiment performed on single crystal SC ice at 185 K in the 14 mm orifice reactor. Before opening the sample compartment at $t = 22$ s, the level of contaminants (Br_2O, HOBr) flowing out of the $BrONO_2$ storage vessel is low. Right after the opening of the sample compartment, the $BrONO_2$ (solid line) signal immediately drops and the reaction leads to rapid formation of HOBr (circles) and Br_2O (triangles). After correction of the $BrONO_2$ MS signal at *m*/*e*

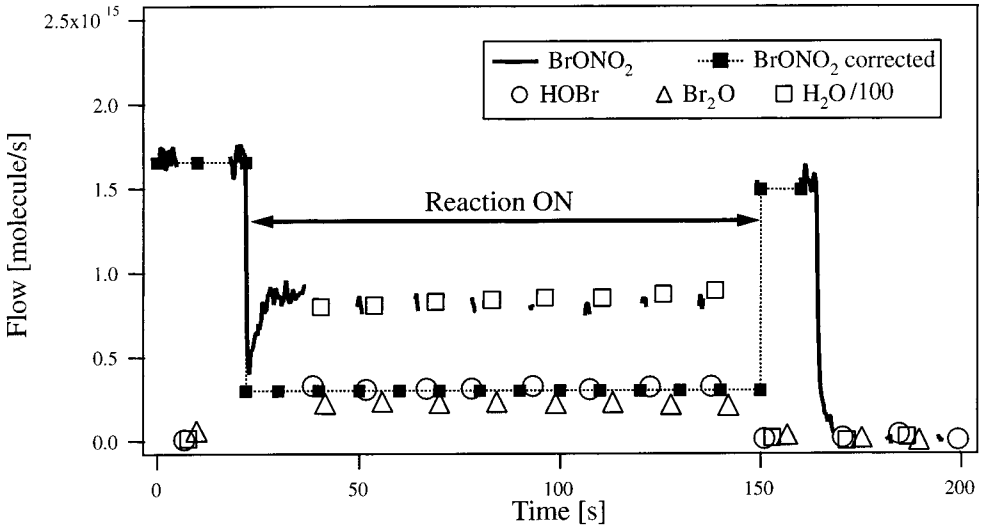

Figure 5. Steady-state experiments of $BrONO_2$ (solid line) on SC ice at 185 K performed in the 14 mm aperture reactor. $BrONO_2$, monitored at *m*/*e* 95, has been corrected for the Br_2O (*m*/*e* 176) contribution at *m*/*e* 95. HOBr (○), monitored at *m*/*e* 98, and Br_2O (△) appear promptly when the plunger is lifted. Note that the H_2O signal (□) has been divided by 100.

95 for the Br_2O contribution, one does not observe saturation of $BrONO_2$ uptake on the ice sample, in contrast to $ClONO_2$.[21,32]

A typical pulsed valve (PV) experiment is displayed in Figure 1, where panel a shows the reactant pulses at *m*/*e* 95 and panel b displays the product pulses HOBr (bold line) and Br_2O (thin line). In this PV experiment a systematic correction has been applied to the reactive $BrONO_2$ MS signal whenever Br_2O was observed. The HOBr and Br_2O rise times are 0.08 and 0.18 s, respectively (Figure 1, panel b), clearly indicating that HOBr is the primary product by virtue of its fast rise time. This therefore confirms the existence of a secondary reaction between $BrONO_2$ and HOBr on the ice surface, leading to the formation of Br_2O, reaction 3.

PV and SS experiments did not show any difference in the numerical value of the uptake coefficient of $BrONO_2$ at a fixed temperature and type of ice. All experiments are detailed in Table 4 and are summarized in Table 5. The values are in good agreement with those found in the literature at 190−200 K on C ice.[17,33] No concentration dependence has been observed in the chosen temperature range, thus confirming a rate law first order in $[BrONO_2]$ for its uptake on all types of ice (Table 4).

The mean product yields of the heterogeneous hydrolysis of $BrONO_2$ on fresh, that is, previously not exposed ice, are displayed in Figure 6 as a function of the substrate temperature. The uncertainties in the yields have been estimated to be 40%, primarily resulting from the difficulties to obtain a "clean" source for HOBr and Br_2O for calibration purposes. The HOBr (or Br_2O) source always contains Br_2O (or HOBr) impurities at different concentrations from batch to batch. While the Br_2O yield appears constant, of the order of 20% or so for all temperatures, the HOBr yield increases with increasing temperature, as observed for Br_2O hydrolysis (Figure 4). Thermal desorption experiments (TDE) performed after $BrONO_2$ uptake on C ice revealed the missing HOBr, thus closing the bromine mass balance (Table 4). On B and SC ice the bromine mass balance appears to be open owing to likely diffusion of bromine species into the bulk of the sample.

The Arrhenius representation of k_{uni} displayed in Figure 7 clearly shows three different lines each with a negative temperature dependence depending on the three different types of ice used. At 180 K, the uptake kinetics of $BrONO_2$ on C, B, and SC ice is identical with $\gamma \approx 0.3$ within experimental uncertainty. At $T > 180$ K we observe that the γ values split into three lines and change according to the following sequence for the different types of ice: $\gamma_C > \gamma_B > \gamma_{SC}$ with γ_C (squares) $\approx 1.4\gamma_B$ (triangles). The uptake kinetics of $BrONO_2$ on B and C ice lead to an adsorption activation energy of $E_a = -2.0 \pm 0.2$ kcal/mol. The negative temperature dependence of γ_{SC} is more pronounced than for B and C ice, leading to $E_a = -6.6 \pm 0.3$ kcal/mol. The uptake coefficient γ_{SC} drops from 0.35 at 180 K to 0.02 at 210 K. Because of the slow rate of cooling of H_2O during SC ice generation, it is assumed that the sample surface has a very low surface defect density such as dislocations or cracks[34] compared to B ice. When the number of defects are important, $BrONO_2$ uptake on ice is apparently faster, as is observed in Figure 7, because these surface sites strongly interact with the gas phase. In agreement with these arguments it is not surprising to observe lower γ values on SC than on C ice. However, at 180 K the number of the defects originating from the ice preparation seems to have no influence on the uptake kinetics of $BrONO_2$ because it already is very fast. The difference observed in the γ values of C and B ice may be due to the fact that C ice is more porous than B ice.[29]

We propose that the hydrolysis of $BrONO_2$ occurs through precursor formation similarly to the analogous $ClONO_2/H_2O$-ice system.[21,32] The existence of a precursor in the hydrolysis of $BrONO_2$ is ascertained by the following two observations:

•The negative temperature dependence observed on all types of ice reveals that the hydrolysis of $BrONO_2$ is not an elementary reaction but consists of a complex sequence of reactive events.

•HOBr only begins to appear in the gas phase after a series of several pulses at doses of $< 5 \times 10^{14}$ molecules, indicating the accumulation of an intermediate species on the surface. At higher doses, both HOBr and Br_2O are released into the gas phase right after the first pulse (Figure 1). This experiment has been performed at $T > 200$ K when a substantial fraction of the generated HOBr is expected to desorb.

Gane et al.[14] experimentally identified $H_2OBr^+\cdots NO_3^-$ as a precursor in the hydrolysis of $BrONO_2$ on ice substrates using reflection−absorption infrared spectroscopy (RAIRS), while McNamara and Hillier[15] reached the same conclusion in performing high-level electronic structure calculations. This precursor corresponds to a complex between protonated hypobromous acid stabilized by the nitrate ion. The prompt formation

TABLE 4: Results of the Interaction of $BrONO_2$ on Different Types of Ice Performed in the 14 mm Escape Orifice Reactor: (a) Bulk (B) Ice, (b) Condensed (C) Ice, and (c) Single Crystal (SC) Ice

T [K]	γ_0	k_{uni} [s^{-1}]	flow[a] [molecule/s]	dose[b] [molecules]	η_{HOBr} [c] [%]	η_{Br2O} [c] [%]	η_{HOBr} [d] [%]	η_{Br2O} [d] [%]
				(a) B Ice				
170	0.23	11.5	1.2×10^{15}		3	3	42	16
180	0.29	14.5	1.2×10^{15}		6	7		
180	0.26	13.0	1.2×10^{15}		9	9	35	45
180	0.33	16.5	1.4×10^{15}		8	17		
180	0.23	11.5	2.2×10^{15}		12	11	35	13
180	0.22	11.0	3.6×10^{15}		12	n.o.[e]		
190	0.19	9.5	1.8×10^{15}		6	n.o.		
200	0.14	7.0	1.3×10^{15}					
200[f]	0.17	8.5	1.4×10^{15}		89	7		
200	0.15	7.5	2.1×10^{15}		90	6		
200	0.15	7.5	2.2×10^{15}		40	n.o.		
210	0.14	7.0	1.0×10^{15}		88	16		
210	0.10	5.0	2.7×10^{15}		90	15		
210[f]	0.13	6.5	4.2×10^{15}		85	9		
180[f]	0.24	12.0		2.8×10^{14}	n.o.	n.o		
190	0.21	10.1		4.2×10^{14}	n.o.	n.o		
195	0.15	7.7		4.1×10^{14}	n.o.	n.o		
200	0.14	7.0		3.2×10^{14}	n.o.	n.o		
200	0.14	7.2		3.6×10^{14}	n.o.	n.o		
208	0.12	5.9		2.3×10^{14}	n.o.	n.o		
210	0.08	3.8		5.4×10^{14}	50	25		
210	0.11	5.3		7.8×10^{14}	42	21		
				(b) C Ice				
180	0.34	17.0	6.7×10^{14}		5	20	58	34
180[f]	0.35	17.5	1.3×10^{15}		2	21	28	28
180	0.34	17.0	3.4×10^{15}		9	17	64	26
190	0.30	15.0	7.0×10^{14}		23	20	45	28
190	0.29	14.5	1.3×10^{15}		14	19	54	30
200	0.21	10.5	1.5×10^{15}		71	15	4	n.o.
200	0.25	12.5	2.0×10^{15}		67	15	6	n.o.
210	0.14	7.0	1.4×10^{15}		84	11	n.o.	n.o.
211	0.15	7.5	3.0×10^{15}		100	n.o.	n.o.	n.o.
180	0.38	19.1		3.4×10^{14}	n.o.	n.o.		
180	0.28	14.0		3.6×10^{14}	n.o.	n.o.		
180	0.34	16.8		2.5×10^{15}	9	n.o.		
190	0.27	13.4		6.6×10^{14}	n.o.	4		
190	0.27	13.5		7.0×10^{14}	4	20		
190	0.21	10.4		2.0×10^{15}	12	n.o.		
200[f]	0.22	11.0		3.0×10^{14}	30	14		
200	0.18	9.0		1.8×10^{15}	16	20		
210	0.16	7.9		7.3×10^{14}	53	30		
210	0.16	7.9		1.2×10^{15}	73	35		
				(c) SC Ice				
180	0.30	15.0	1.2×10^{15}		22	4	31	10
180	0.39	19.5	1.8×10^{15}		23	9		
185	0.22	11.0	1.6×10^{15}		26	13		
190	0.14	7.0	1.0×10^{15}		37	10		
190[f]	0.15	7.5	1.5×10^{15}		61	29		
195	0.10	5.0	1.4×10^{15}		76	15		
200	0.07	3.5	1.7×10^{15}		118	14		
205	0.04	2.0	1.3×10^{15}		78	12		
210	0.022	1.1	1.2×10^{15}		106	10		
210	0.025	1.3	1.4×10^{15}		94	1		

[a] Steady-state experiments. [b] Pulsed valve experiments. [c] HOBr and Br_2O yields during uptake experiments. [d] HOBr and Br_2O yields observed in the gas phase upon thermal desorption experiments (TDE). [e] n.o. = not observed. [f] Experiments performed in the 8 mm escape orifice reactor.

TABLE 5: Initial Uptake Coefficients for $BrONO_2$ on Different Types of Ice Using the 14 mm Orifice Reactor Resulting from SS and PV Experiments and Activation Energy, E_a, [kcal/mol] for the Uptake Rate Coefficient[a]

T [K]	γ_C	γ_B	γ_{SC}
180	0.34 ± 0.03	0.26 ± 0.04	0.35 ± 0.05
190	0.27 ± 0.03	0.20 ± 0.01	0.145 ± 0.005
200	0.22 ± 0.03	0.15 ± 0.01	
210	0.15 ± 0.01	0.11 ± 0.02	0.024 ± 0.001
E_a	-2.0 ± 0.2	-2.1 ± 0.2	-6.6 ± 0.3

[a] Using $\omega(BrONO_2) = 34\sqrt{T/M}$ s^{-1} (Table 2).

of HOBr suggests that $H_2OBr^+\cdots NO_3^-$ is less stable than $H_2OCl^+\cdots NO_3^-$ for the corresponding chlorine system in the same temperature range.[21,32]

If $BrONO_2$ adsorption occurs on a surface that previously has taken up a few monolayers of HNO_3 from the gas phase, the rate of uptake is unchanged compared to γ values obtained on clean fresh B ice. However, the rate of HOBr production on a contaminated ice substrate is delayed with respect to a clean ice substrate. It takes approximately 1 min for HOBr to reach steady state in the temperature range 180−210 K after the opening of the sample compartment (dashed line in Figure 8) as opposed to a clean ice surface (solid line in Figure 8). This shows that the presence of HNO_3 has a marked effect on the rate of production of HOBr by stabilizing the precursor and thus delaying the observation of HOBr in the gas phase. Less H_2O is available to hydrolyze $BrONO_2$ to HOBr, as has been already observed in the study of the heterogeneous reaction of $BrONO_2$ on alkali salts.[22]

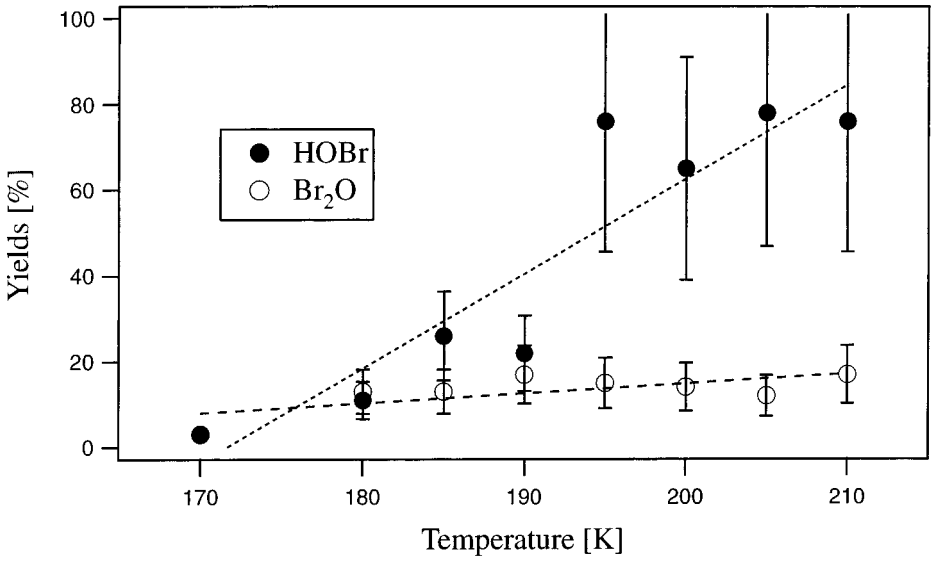

Figure 6. HOBr (●) and Br_2O (○) yields resulting from the heterogeneous reaction of $BrONO_2$ on pure ice of all types (B, C, SC).

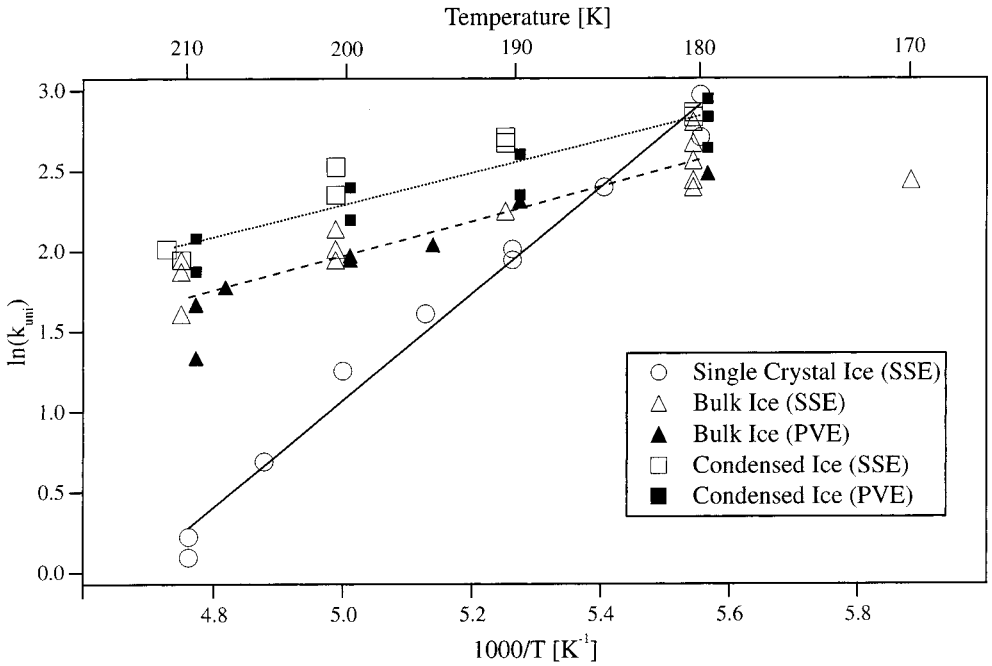

Figure 7. Arrhenius representation of the uptake rate constant for the hydrolysis of $BrONO_2$ on B ice (triangles), C ice (squares), and SC ice (circles), obtained in PV (solid symbols) and SS experiments (open symbols).

$BrONO_2$ Uptake on Ice Doped with HBr. The presence of HBr on the ice sample leads to the competition between the hydrolysis scheme (reactions 13 and 3) and the following reaction:

$$BrONO_2 + HBr \rightarrow Br_2 + HNO_3 \qquad (14)$$

Figure 9 displays a typical SS experiment on B ice performed at 190 K in the 14 mm orifice reactor. When the sample compartment is opened, one observes a rapid drop of the $BrONO_2$ MS signal (squares) at *m*/*e* 95 correlated with an initially slow production of Br_2 (triangles down), which is the primary product. The $BrONO_2$ signal has been corrected for the contribution of Br_2O at *m*/*e* 95. When the production of Br_2 begins to decrease, a slow release of HOBr and Br_2O appears in the gas phase, confirming the competition between reaction 14 and the hydrolysis of $BrONO_2$, reactions 13 and 3. In contrast to SS experiments no HOBr and Br_2O have been observed in PV experiments. The only observed product was Br_2, as displayed in Figure 10 (right panel). The net Br_2 production has been obtained by subtraction of the pulse obtained with the sample compartment closed (reference pulse) from the reactive pulse (sample compartment open).

As displayed in Figure 9, the production yields of HOBr and Br_2O are small, of the order of 10% or so taken together. This may be due to the fact that HOBr reacts on ice substrates containing HBr to Br_2, which is released[20] into the gas phase according to reaction 15.

$$HOBr + HBr \rightarrow Br_2 + H_2O \qquad (15)$$

The uptake kinetics of HOBr in this latter reaction is fast with a constant uptake coefficient of $\gamma = 0.3$ in the temperature range 180−195 K.[31] The slow rise in the formation of Br_2 observed in Figure 9 is due to the rate-limiting production of HOBr adsorbed on the ice surface, reaction 13. When sufficient

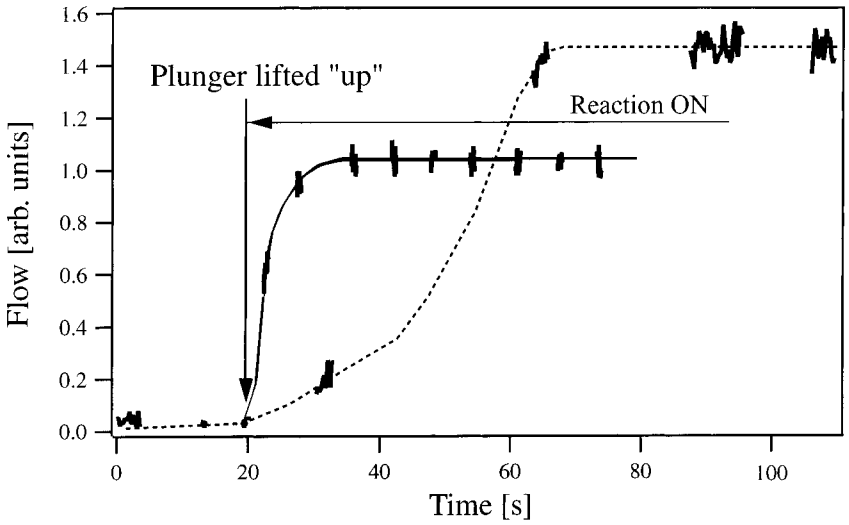

Figure 8. HOBr (*m/e* 98) production from SS experiments on fresh B ice (solid line) and on B ice doped with 1.3×10^{16} HNO_3 molecules (dashed line) at 180 K in the 14 mm orifice reactor. Delayed rate of production of HOBr is observed when HNO_3 is adsorbed prior to the uptake experiment.

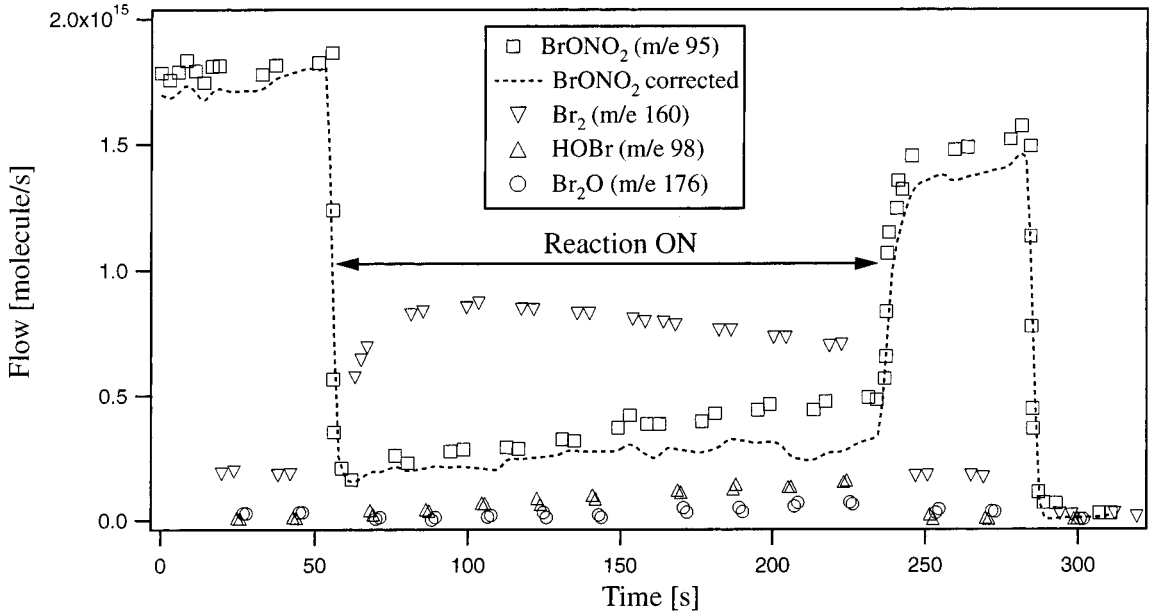

Figure 9. SS experiment of $BrONO_2$ on B ice doped with 1.1×10^{18} HBr molecules at 190 K in the 14 mm orifice reactor. The MS signal of $BrONO_2$ (□), monitored at *m/e* 95, has been corrected (dashed line) for the contribution of Br_2O (○, *m/e* 176) at *m/e* 95. The main product, Br_2 (▽, *m/e* 160), appears in a yield of 43%, the yields of the hydrolysis products, HOBr (△) and Br_2O, are 8 and 4%, respectively.

HOBr is formed in the condensed phase, reaction 15 takes place, producing Br_2. HOBr is efficiently consumed by HBr in reaction 15, which reduces the rate of reaction 3, thus leading to the small amount of Br_2O observed in Figure 9.

The uptake coefficients are summarized in Table 6. No difference between SS and PV experiments have been observed on C ice. For a fixed temperature, no difference between B and C ice has been observed as far as the uptake kinetics of $BrONO_2$ is concerned. No concentration dependence of the uptake kinetics of $BrONO_2$ has been noted, which leads to a rate law for the uptake first order in $[BrONO_2]$.

In contrast to the $ClONO_2$ + HBr/ice reactive system,[35] we observe a negative temperature dependence for the rate constant of reaction 14 in the range 180−210 K. The Arrhenius representation displayed in Figure 11 reveals a less pronounced dependence, as has been observed for the hydrolysis of $BrONO_2$ on pure ice, reaction 13 (Figure 7). The resulting activation energy for the reaction of $BrONO_2$ with HBr is $E_a = -1.2 \pm 0.2$ kcal/mol, which confirms that Br_2 formation in reaction 14 does not occur through an elementary reaction.

Conclusions and Atmospheric Implications

Br_2O hydrolysis on ice substrates occurs rapidly in the chosen temperature range of 180−210 K. The uptake kinetics is fast in contrast to the analogous Cl_2O/H_2O where no heterogeneous interaction has been observed.[21] At a fixed temperature, the rate law is first order in $[Br_2O]$. HOBr has been observed as the sole product of the Br_2O hydrolysis and the release of HOBr into the gas phase is prompt. The observed temperature dependence of the initial and steady-state rate constant leads to an activation energy E_a for heterogeneous hydrolysis of 0.0 ± 2.0 kcal/mol.

In the gas phase the hydrolysis of Br_2O is an equilibrium reaction,[19] which may, however, take place at the walls of the reaction vessel under most experimental conditions. The equi-

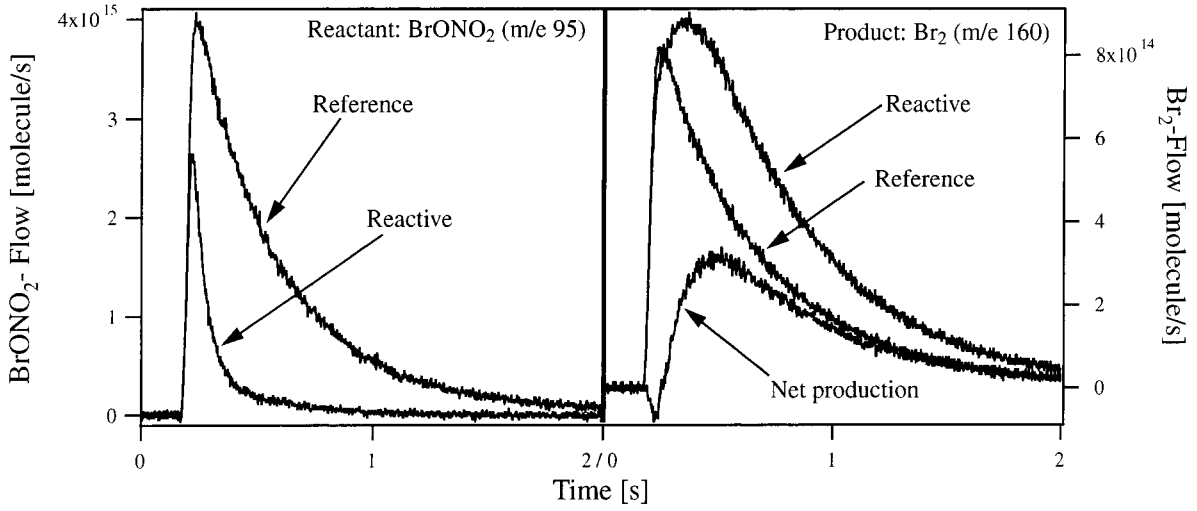

Figure 10. PV experiment of $BrONO_2$ on C ice doped with 1.1×10^{18} molecules of HBr at 180 K in the 14 mm orifice reactor. $BrONO_2$ (left panel), monitored at *m*/*e* 95, has not been corrected, because no Br_2O has been observed. The main product, Br_2, whose rise time is 0.35 s (right panel, *m*/*e* 160), appears in a yield of 17%. Neither HOBr nor Br_2O, have been observed.

TABLE 6: Initial Uptake Coefficients γ^{HBr} for $BrONO_2$ on C and B Ice Doped with HBr Using the 14 mm Orifice Reactor Resulting from SS and PV Experiments (Averaged) Compared to $\gamma_C^{H_2O}$ on Pure Ice (Table 5)

T [K]	γ^{HBr}	N(HBr)[a] [molecules]	$\gamma_C^{H_2O}$
180	0.30 ± 0.03	5.5×10^{17} to 4.7×10^{18}	0.34 ± 0.03
190	0.28 ± 0.03	approx 1.0×10^{18}	0.27 ± 0.03
200	0.23 ± 0.03	$(1.0-4.5) \times 10^{18}$	0.22 ± 0.03
210	0.17 ± 0.02	approx 1.0×10^{18}	0.15 ± 0.01

[a] N(HBr) corresponds to the amount of HBr taken up prior the uptake experiments.

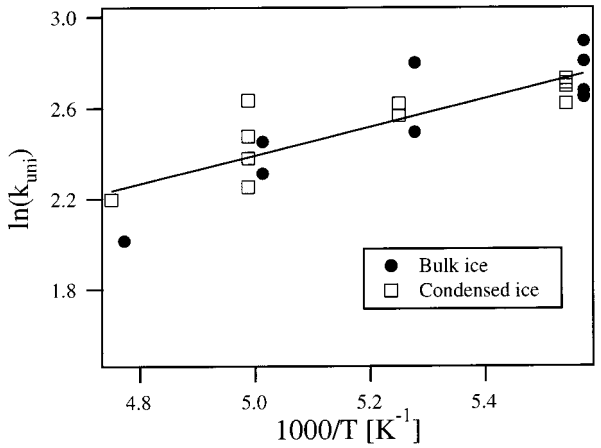

Figure 11. Arrhenius representation of the rate constant of the reaction of $BrONO_2$ on B and C ice doped with HBr. The activation energy for the heterogeneous reaction of $BrONO_2$ with HBr adsorbed on ice is $E_a = -1.2 \pm 0.2$ kcal/mol.

librium is shifted in favor of adsorbed HOBr for reaction on ice surfaces at low temperatures (180−210 K), in agreement with the results of Gane.[36] Due to low atmospheric concentrations the HOBr self-reaction to Br_2O will be slow. As only the reverse reaction occurs ($Br_2O + H_2O \rightarrow 2HOBr$), one may conclude that there will be no significant concentration of Br_2O in the atmosphere, also because of its anticipated photolytic instability under UT/LS conditions.

$BrONO_2$ hydrolysis has been measured on B-, C-, and SC ice in the temperature range 180−210 K. On all types of ice we observe a prompt HOBr and Br_2O production. At a fixed temperature the rate law for $BrONO_2$ uptake on ice is first order in $[BrONO_2]$. The observed negative temperature dependence leads to an activation energy E_a for heterogeneous hydrolysis of $BrONO_2$ on pure ice of -2.0 ± 0.2, -2.1 ± 0.2, and -6.6 ± 0.3 kcal/mol on C, B, and SC ice, respectively, revealing different uptake kinetics of $BrONO_2$ on the three different types of ices used in this study. The efficiency of the $BrONO_2$ hydrolysis allows HOBr to become the most important form of nighttime bromine in the stratosphere.

The presence of HBr on/in the ice of the order of 10^{18} molecules condensed prior to $BrONO_2$ uptake leads to the formation of Br_2, followed by HOBr and Br_2O production once the HBr supply on the ice is waning. The observed reaction kinetics of $BrONO_2$ with HBr is identical to the one for hydrolysis of $BrONO_2$ on pure ice (Table 6), suggesting that adsorbed HBr has apparently no influence on the uptake kinetics. This means that the rate of reaction is faster than the rate of uptake, which is rate limiting. PV experiments show a Br_2 rise time of 0.35 s (Figure 10), which is between 2 and 4 times larger compared to the rise time of Br_2O and HOBr, respectively, observed in PV experiments of $BrONO_2$ on pure ice. This rise time of 0.35 s is larger compared to 0.08 s for the HOBr rise time, if the reaction occurs directly between $BrONO_2$ and HBr. In agreement with these observations we propose the following reaction scheme for the interaction of $BrONO_2$ on ice doped with HBr:

$$BrONO_2(g) + H_2O(s) \rightarrow HOBr(c) + HNO_3(c) \quad (16)$$

$$HOBr(c) + HBr(c) \rightarrow Br_2(g) + H_2O(s) \quad (17)$$

The first step (reaction 16) corresponds to the hydrolysis of $BrONO_2$ and leads to the formation of condensed-phase HOBr, which then reacts with HBr to produce gaseous Br_2 (reaction 17). In conclusion, the interaction of $BrONO_2$ with HBr occurs stepwise and is quite different from the analogous chlorinated system $ClONO_2$/HCl, which goes through a direct interfacial reaction leading to the prompt release of Cl_2 in the gas phase, as pointed out by Oppliger et al.[21]

Acknowledgment. Funding for this work was provided by the Office Fédéral de l'Enseignement et de la Science (OFES) in the framework of the subprojects COBRA and CUTICE of the EU program "Environment and Climate". We thank Prof.

Hubert van den Bergh for his lively interest and input. We also thank Dr. M. P. Gane for sending us selected chapters of his Ph.D. thesis and an anonymous referee for a particularly pertinent question.

References and Notes

(1) McElroy, M. B.; Salawitch, R. J.; Wofsy, S. C.; Logan, J. A. *Nature* **1986**, *321*, 759.
(2) Solomon, S.; Garcia, R. R.; Rowland, F. S.; Wuebbles, D. J. *Nature* **1986**, *321*, 755.
(3) Cicerone, R. J. *Science* **1987**, *237*, 35.
(4) Turco, R.; Toon, O. B.; Hamill, P. *J. Geophys. Res.* **1989**, *94*, 16493.
(5) Henderson, G. S.; Evans, W. F. J.; MccConnell, J. C. *J. Geophys. Res.* **1990**, *95*, 1899.
(6) Lary, D. J. *J. Geophys. Res.* **1996**, *101*, 1505.
(7) Tie, X. X.; Brasseur, G. *Geophys. Res. Lett.* **1996**, *23*, 2505.
(8) Thorn, R. P.; Daykin, E. P.; Wine, P. H. *Int. J. Chem. Kinet.* **1993**, *25*, 521.
(9) Spencer, J. E.; Rowland, F. S. *J. Phys. Chem.* **1978**, *82*, 7.
(10) Burkholder, J. B.; Ravishankara, A. R.; Solomon, S. *J. Phys. Chem.* **1995**, *100*, 16793.
(11) Harwood, M. H.; Burkholder, J. B.; Ravishankara, A. R. *J. Phys. Chem. A* **1998**, *102*, 1309.
(12) Soller, R.; Nicovich, J. M.; Wine, P. H. *J. Phys. Chem. A* **2001**, *105*, 1416.
(13) Goldfarb, L.; Harwood, M. H.; Burkholder, J. B.; Ravishankara, A. R. *J. Phys. Chem. A* **2001**, *105*, 4002.
(14) Gane, M. P.; Williams, N. A.; Sodeau, J. R. *J. Phys. Chem. A* **2001**, *105*, 4002.
(15) McNamara, J. P.; Hillier, I. H. *J. Phys. Chem. A* **2001**, *105*, 7011.
(16) Hanson, D. R.; Ravishankara, A. R. *Geophys. Res. Lett.* **1995**, *22*, 385.
(17) Hanson, D. R.; Ravishankara, A. R.; Lovejoy, E. R. *J. Geophys. Res.* **1996**, *101*, 9063.
(18) Allanic, A.; Oppliger, R.; Rossi M. J. *J. Geophys. Res.* **1997**, *102*, 23529.
(19) Orlando, J. J.; Burkholder, J. B. *J. Phys. Chem.* **1995**, *99*, 1143.
(20) Abbatt, J. P. D. *Geophys. Res. Lett.* **1994**, *21*, 665.
(21) Oppliger, R.; Allanic, A.; Rossi, M. J. *J. Phys. Chem. A* **1997**, *101*, 1903.
(22) Aguzzi, A.; Rossi M. J. *Phys. Chem. Chem. Phys.* **1999**, *1*, 4337.
(23) Ennis, C. A.; Birks, J. W. *J. Phys. Chem.* **1985**, *89*, 186.
(24) Schreiner, J.; Voigt C.; Kohlmann, A.; Arnold, F.; Mauersberger, K.; Larsen, N. *Science* **1999**, *283*, 968.
(25) Caloz, F.; Fenter F. F.; Tabor K.; Rossi M. J. *Rev. Sci. Instrum.* **1997**, *68*, 3172.
(26) Tevault, D. E.; Walker, N.; Smardzewski, R. R.; Fox, W. B. *J. Phys. Chem.* **1978**, *82*, 2733.
(27) Wilson, W. W.; Christe, K. O. *Inorg. Chem.* **1987**, *26*, 1573.
(28) Knight, C. A. *J. Glaciol.* **1996**, *42*, 585.
(29) Chaix, L.; van den Bergh, H.; Rossi, M. J. *J. Phys. Chem. A* **1998**, *102*, 10300.
(30) Chu, L.; Chu, L. T. *J. Phys. Chem. A* **1999**, *103*, 8640.
(31) Chaix, L.; Allanic, A.; Rossi, M. J. *J. Phys. Chem. A* **2000**, *104*, 7268.
(32) Leu, M. T.; Moore, S. B.; Keyser, L. F. *J. Phys. Chem.* **1991**, *95*, 7763.
(33) Hanson, D. R.; Ravishankara, A. R. In *The Tropospheric Chemistry of Ozone in the Polar Regions*; Niki, H., Becker, K. H., Eds.; NATO ASI Series; NATO: Dordrecht, The Netherlands, 1993; No. 17, p 281.
(34) Hobbs, P. V. *Ice Physics*; Clarendon Press: Oxford, U.K., 1974.
(35) Allanic, A.; Rossi M. J. *J. Geophys. Res.* **2000**, *104*, 18689.
(36) Gane, M. P. Ph.D. Thesis, University of East Anglia, 2000.
(37) Thorn, R. P.; Monks, P. S.; Stief, L. J.; Kuo, S.-C.; Zhang, Z.; Klemm, R. B. *J. Phys. Chem.* **1996**, *100*, 12199.
(38) Lock, M.; Barnes, R. J.; Sinha, A. *J. Phys. Chem.* **1996**, *100*, 7972.
(39) Thorn, R. P.; Stief, L. J.; Kuo, S.-C.; Klemm, R. B. *J. Phys. Chem.* **1996**, *100*, 14178.
(40) Cox, J. D., Wagman, D. D., Medvedev, V. A., Eds. *CODATA Key Values for Thermodynamics*; Hemisphere: New York, 1989.
(41) *Chemical Kinetics and Photochemical Data for Use in Stratospheric Modeling*; Evaluation Number 12; JPL Publication: Pasadena, CA, 1997.